Dehydrogenation of Ethylbenzene over Spinel Oxides

N. John JEBARATHINAM, M. ESWARAMOORTHY, and V. KRISHNASAMY*
Department of Chemistry, Anna University, Madras 600025, India
(Received May 9, 1994)

$NiCr_2O_4$, $ZnCr_2O_4$, $CuCr_2O_4$, $CuAl_2O_4$, and $CuFe_2O_4$ were prepared and characterized by XRD, DRS, and IR and by measurements of surface area, acidity, and electrical conductivity. XRD analysis indicates, that chromites, aluminate, and ferrite have normal, partially inversed, and inversed spinel structure, respectively. Electrical conductivity measurements show the existence of pair localized ions which are positive in chromites and negative both in aluminate and ferrite. The catalytic activity of chromites and aluminate are comparable and higher than that of ferrite in the conversion of ethylbenzene under all experimental conditions. However selectivity to styrene formation follows in the following order: ferrite>chromites>aluminate. The ratio of B/T (benzene/toluene) is more than unity over aluminate and less than unity over chromites and ferrite. Evolution of CO_2 remains constant while that of C_2H_4 increased with increase in temperature keeping its formation always higher over aluminate. Measurements of acidity and basicity by TGA show the presence of basic sites on chromites, acidic sites on aluminate, and both sites on ferrite which influence the conversion of ethylbenzene to various products. The XRD pattern of spent catalysts indicate the appearance of metallic copper phase over $CuCr_2O_4$, $CuFe_2O_4$, and $CuAl_2O_4$. In the case of $NiCr_2O_4$ and $ZnCr_2O_4$ no significant difference is observed.

The catalytic dehydrogenation of ethylbenzene is an industrially important process for the manufacture of styrene. Iron(III) oxide promoted with alkali metal ions was used in most of the industrial processes.[1—3] Spinel oxides with a general formula AB_2O_4, are reported to be thermally stable and they maintain enhanced and sustained activities for variety of industrially important reactions like decomposition of nitrous oxide,[4] oxidation and dehydrogenation of hydrocarbons,[5] low temperature methanol synthesis,[6] oxidation of carbon monoxide and hydrocarbon,[7] and oxidative dehydrogenation of butanes.[8] In the present investigation a series of spinel oxides such as $NiCr_2O_4$, $ZnCr_2O_4$, $CuCr_2O_4$, $CuAl_2O_4$, and $CuFe_2O_4$ which posses same structure but different co-ordination of metallic ions, were prepared, characterized and their catalytic activity for the dehydrogenation of ethylbenzene to styrene were investigated.

Experimental

Preparation of Catalysts. A mixture of 10% solution of metal nitrates was taken in the ratio of $M^{3+}:M^{2+}=2:1$ and the mixture was heated to 333—353 K. To this hot mixture, a 5% ammonia solution was added drop wise with constant and uniform stirring to maintain a constant pH of 6.2, 6.5, 7.0, 7.5, and 8 for $CuFe_2O_4$, $CuCr_2O_4$, $ZnCr_2O_4$, $CuAl_2O_4$, and $NiCr_2O_4$ respectively. The mixture was digested for another 2 h at 353 K for completion of precipitation. The precipitates were filtered, washed and dried in air at 378 K for 12 h and calcined at 1073 K.[9,10]

ICP Analysis. One tenth gram of each sample was heated in 5—10 ml of perchloric acid and the solution was made up to 100 ml. The metal concentration was estimated by ICP (Minitorch 3410) analysis and the data are given in Table 1.

X-Ray Analysis. X-Ray powder diffraction patterns were recorded on Philips X-ray diffractometer, (PW 1050) with microprocessor controller using Cu $K\alpha$ radiation (λ= 0.15405 nm). X-Ray pattern of all spinels are shown in Fig. 1. The lattice parameters are given in Table 2.

Table 1. Chemical Analysis of the Prepared Spinels

Compd	Me^{3+}/ %wt		Me^{2+}/ %wt	
	Calcd	Exptl	Calcd	Exptl
$NiCr_2O_4$	45.88	46.46	25.89	26.39
$ZnCr_2O_4$	44.56	45.58	28.01	29.13
$CuCr_2O_4$	44.91	45.44	27.45	27.54
$CuFe_2O_4$	46.69	45.93	26.56	25.82
$CuAl_2O_4$	29.73	29.81	35.01	34.98

DRS Analysis. Diffuse reflectance spectra were measured at room temperature in the range 300—1600 nm (carry-2390 spectrophotometer) using freshly prepared MgO as standard[11] and the data are plotted inFig. 2.

IR Study. Two to four milligrams of each substance were pressed with 200 mg of KBr. The spectra were recorded in Hitachi-5890 IR spectrophotometer in the region 250—1400 cm^{-1} and are shown in Fig. 3.

Electrical Conductivity Measurements. The elec-

Table 2. Activation Energy (E_σ), Seeback Coefficient (α), Lattice Parameter (a), and Surface Area (S) of the Spinels

Spinels (Color)	E_σ eV	α $\mu V\,°C^{-1}$	Type	a Å	S $m^2\,g^{-1}$
$NiCr_2O_4$ (green)	0.746	+346	p	8.302	13.36
$ZnCr_2O_4$ (grey)	0.976	+ 62	p	8.314	12.94
$CuCr_2O_4$ (bluish black)	0.864	+186	p	8.552	9.50
$CuFe_2O_4$ (black)	1.072	−126	n	8.350	11.60
$CuAl_2O_4$ (black)	1.540	− 26	n	8.045	30.49

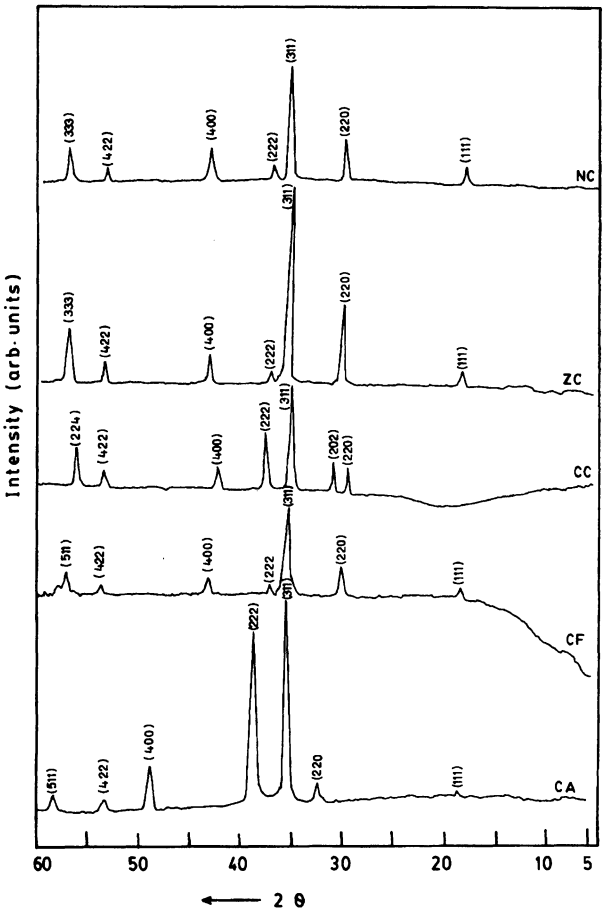

Fig. 1. X-Ray diffractogram.

trical conductivity of the spinels were measured using two probe conductivity cell in the temperature range 303—773 K. A cyclinderical catalyst pellet of 10 mm dia. is pressed firmly between two spring loaded platinum foil (15 mm×15 mm×0.5 mm) fused at the end of pyrex glass tube. The sample holder assembly was placed at the center of a tubular furnace which was heated electrically. A Chromel–Alumel thermocouple was used to measure the temperature of the sample. The activation energy for electrical conduction (E_σ) were obtained from the slope of the plot of $\log\sigma$ vs. $1/T$. The nature of charge carriers (holes or electrons) was determined by checking the sign of the thermoelectric (Seebeck) potential (α).[12] For this purpose the following modification in the conductivity measuring apparatus was made. An auxillary heating element was wound over a silica tube and kept at one end of the conductivity cell containing the catalyst pellet. After equilibrating the sample at each temperature for 15 min, the auxillary heater was switched on and a temperature difference of 10 K was maintained between the sample ends. After a steady state had been attained the Seebeck potential was measured using a d.c. microvoltmeter. In this way, Seebeck potential had been measured at various temperatures.. The values of E_σ and α are given in Table 2.

Surface Area Analysis. The specific surface area of catalysts was determined by BET method using a Carlo Erba Sorptometric instrument. The values are included in Table 2.

Acidity and Basicity Measurements. The acidity and basicity of the catalysts were measured by butylamine and acetic acid adsorption[13] respectively. The catalyst in a desiccator, was saturated with butylamine/acetic acid vapors at room temperature for 48 h. Then, the weight loss of the adsorbed sample was measured by a TGA (Mettler-TA 2000 Series) operating from 313—873 K heating at a rate of 20 K min^{-1}. The weight loss between 423—573, 574—723, and 724—873 K are considered to be week, medium, and strong sites respectively and the values are given in Table 3.

Apparatus and Procedure. The catalytic reaction was carried out in the temperature range 763 to 853 K at WHSV of 2 h^{-1} in the vapor phase using an integral flow type reactor consisting of a quartz glass tube (8.0 mm i.d.) in which a sintered porcelin disc was sealed in the middle of the reactor to support the catalyst. The temperature was measured by a thermocouple placed in the centre of the catalyst bed. Before each catalytic run, the catalyst was heated under flowing air at 773 K and allowed to remain at that temperature for 6 h. After this period, the catalyst was heated or cooled to the reaction temperature (763—853 K) and air was replaced by reactant ethylbenzene using infusion pump that could be operated at different flow rates. The products collected for the first 30 min were discarded and analysis was made only of the products collected after this time. This was done to ensure the attainment of steady state for the reaction over the catalyst and also to eliminate temperature fluctuations. The liquid products were found to contain styrene, benzene, toluene, and unreacted ethylbenzene by Gas Chromatographic analysis (Hewlett–Packard-5890) and the results are illustrated in Table 4. The gaseous products were analyzed by Orsat gas analyser and the data are given in Table 4.

At the end of each run, the reactor was flushed with nitrogen, to remove the adsorbed hydrocarbon, polymer etc. Air freed from CO_2 by passing through alkali and an activated silica gel tower, was allowed to pass through the reactor at 773 K. The coke deposited on the catalyst was oxidized to oxides of carbon. The gaseous mixture was subsequently passed through platinized asbestos kept at 773 K, where CO was oxidized to CO_2 which was absorbed in alkali of known concentration. This operation was continued for 6 h and at the end of this period, the alkali solution was back titrated. From the difference in the titre values the percentage of carbon was estimated. The values obtained at different temperatures are given in Table 5.

Results and Discussion

X-Ray powder diffraction patterns (Fig. 1) of all the catalysts show the formation of single spinel phase. $NiCr_2O_4$ (NC), $ZnCr_2O_4$ (ZC), $CuAl_2O_4$ (CA), and $CuFe_2O_4$ (CF) are crystallized in cubic symmetry whereas $CuCr_2O_4$ (CC) has tetragonally distorted structure. The distribution of cations at tetrahedral (T) and octahedral (O) sites is determined by comparing the calculated intensity ratios I_{220}/I_{422} and I_{422}/I_{400} for different possible models of cation distribution in each spinel with those of the observed intensity ratios. To calculate the relative integrated intensity for the planes (220), (422), and (400), sensitive to the distribution of cations at the tetrahedral sites, the equation

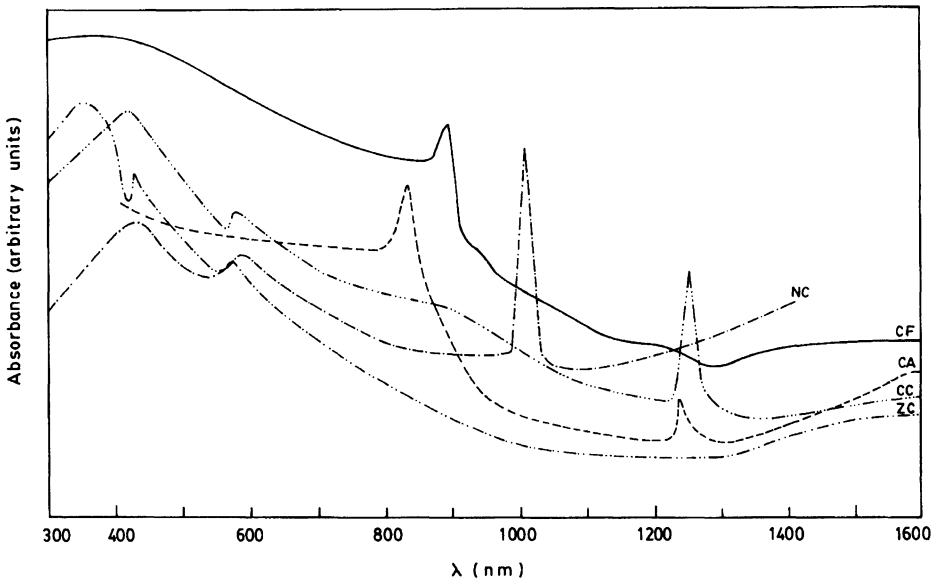

Fig. 2. Diffuse reflectance spectrum.

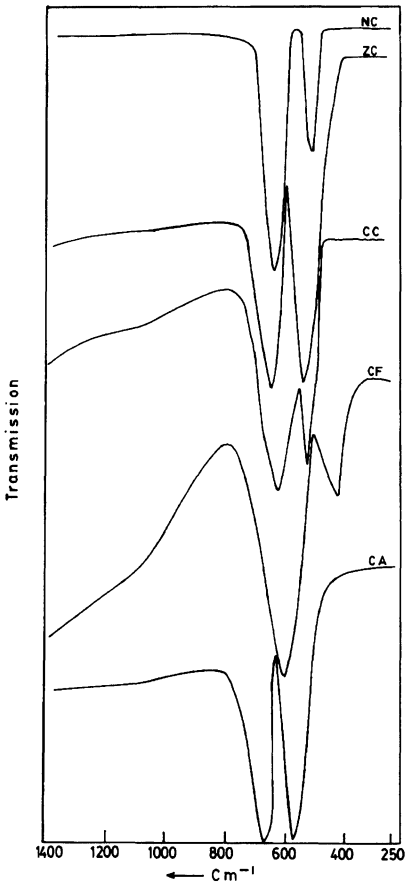

Fig. 3. IR spectra.

$$I_{hkl} = \frac{1 + \cos^2 2\theta}{\sin^2 \theta \cos \theta} |F|^2 P$$

suggested by Burger[14] is used, in which the notation has its usual meanings. The atomic scattering powers for various ions are taken from literature.[15] From this study the ionic configuration of the spinels used in this investigation are as follows.

Spinels	Cation at	
	T site	O site
$NiCr_2O_4$	Ni^{2+}	$2Cr^{3+}$
$ZnCr_2O_4$	Zn^{2+}	$2Cr^{3+}$
$CuCr_2O_4$	Cu^{2+}	$2Cr^{3+}$
$CuAl_2O_4$	$0.65Cu^{2+}$, $0.35Al^{3+}$	$0.35Cu^{2+}$, $1.65Al^{3+}$
$CuFe_2O_4$	Fe^{3+}	Cu^{2+}, Fe^{3+}

The reflectance spectra obtained (Fig. 2) for $NiCr_2O_4$, $ZnCr_2O_4$, and $CuCr_2O_4$ are in accordance to those reported in the literature.[16—18] Freeman and Friedman[19] pointed out that Cu^{2+} at octahedral co-ordination is found absorbing around 830 nm and at tetrahedral co-ordination around 1250 nm. The spectra for $CuCr_2O_4$, $CuFe_2O_4$, and $CuAl_2O_4$ show that the absorption bands corresponding to tetrahedral Cu^{2+} for $CuCr_2O_4$, octahedral Cu^{2+} for $CuFe_2O_4$, and both tetrahedral and octahedral Cu^{2+} for $CuAl_2O_4$. These observations further confirm that they are normal, inversed and partially inversed spinels respectively.

The IR absorption bands (Fig. 3) observed for chromites in the ranges 500—540 and 620—650 cm^{-1} are assigned to the Cr–O and M–O vibrations respectively. The absorption bands observed in the region 400—700 cm^{-1} are characteristics of $CuFe_2O_4$ and $CuAl_2O_4$ with spinel structure.[20]

Seebeck potential (α) measurements show that chromites are p-type while aluminate and ferrite are n-type semiconductors. In chromites $Cr^{3+} \rightleftharpoons Cr^{4+}$ exchange pair is generated in which Cr^{3+} and Cr^{4+} ions have $3d^3$ and $3d^4$ configurations respectively. Between them Cr^{3+} is more stable than Cr^{4+}. Consequently the pair ($Cr^{3+} \rightleftharpoons Cr^{4+}$) need one electron for the conversion of less stable Cr^{4+} to more stable Cr^{3+} and thus it has positive charge and therefore the conductivity is of p-type in chromites. In the case of copper ferrite and copper aluminate, the exchange pair of ions are

Table 3. The Acidity and Basicity Data[a)]

Catalyst	Acidity/mequiv $g^{-1} \times 10^{-1}$				Basicity/mequiv $g^{-1} \times 10^{-1}$			
	1	2	3	4	1	2	3	4
$NiCr_2O_4$	0.6	2.1	0.8	3.5	0.4	1.9	5.1	7.4
$ZnCr_2O_4$	0.7	1.9	0.6	3.2	0.3	1.8	5.8	7.9
$CuCr_2O_4$	0.5	0.6	2.6	3.7	0.3	2.3	4.5	7.1
$CuAl_2O_4$	0.6	1.2	3.4	5.2	0.2	2.0	2.4	4.6
$CuFe_2O_4$	0.6	1.0	8.2	9.8	0.2	1.1	1.5	2.8

a) 1. Weak sites; 2. Medium sites; 3. Strong sites; 4. Total sites.

Table 4. Distribution of Products (mol%) over Spinels[a)]

Product distribution	$NiCr_2O_4$				$ZnCr_2O_4$				$CuCr_2O_4$				$CuFe_2O_4$				$CuAl_2O_4$			
	1	2	3	4	1	2	3	4	1	2	3	4	1	2	3	4	1	2	3	4
Styrene	16.2	27.1	34.2	35.1	14.1	22.7	30.4	31.8	15.2	25.4	32.5	33.1	4.9	8.2	17.2	23.1	8.4	12.5	21.1	24.6
Toluene	0.8	1.4	4.6	12.8	0.7	1.2	3.1	9.8	1.2	4.1	8.3	14.9	0.2	0.4	1.3	1.9	3.0	8.1	12.2	17.1
Benzene	0.4	1.1	1.7	8.2	0.4	0.9	1.4	6.9	0.9	3.2	4.9	13.2	0.1	0.2	0.7	1.1	12.2	14.3	18.8	22.5
Ethylene	—	0.3	0.7	2.1	—	0.4	0.9	1.9	0.5	0.9	2.4	5.9	—	—	—	0.9	5.2	6.7	6.8	7.2
Carbon dioxide	0.4	0.5	0.5	0.6	0.7	0.7	0.8	0.8	0.7	0.8	0.8	0.9	0.5	0.7	0.6	0.6	0.5	0.6	0.7	0.7
EB conversion	17.5	29.8	41.1	56.2	15.2	25.0	35.0	48.9	17.5	33.0	46.0	61.4	5.2	8.9	19.4	26.5	23.8	35.0	53.3	64.5
Styrene selectivity	92.6	90.1	83.2	62.5	92.3	90.8	86.9	65.0	86.9	77.0	70.7	54.0	94.2	92.1	88.7	87.1	35.3	35.7	39.6	38.1

a) 1. 763 K; 2. 793 K; 3. 823 K; 4. 853 K.

Table 5. Carbon Estimation

Catalysts	Carbon content/wt%			
	763 K	793 K	823 K	853 K
$NiCr_2O_4$	0.34	0.81	1.21	2.70
$ZnCr_2O_4$	0.46	0.75	1.10	2.90
$CuCr_2O_4$	0.50	0.92	1.30	4.20
$CuAl_2O_4$	2.32	3.50	4.10	5.20
$CuFe_2O_4$	0.10	0.41	0.82	1.80

($Fe^{2+} \rightleftharpoons Fe^{3+}$) and ($Cu^{+} \rightleftharpoons Cu^{2+}$) respectively in which the iron(III) and copper(II) ions are the stable species. To obtain these species Fe^{2+} in ($Fe^{2+} \rightleftharpoons Fe^{3+}$) and Cu^{+} in ($Cu^{+} \rightleftharpoons Cu^{2+}$) should release an electron and thus the pairs have negative charge. Consequently the conductivity is of n-type in copper ferrite and copper aluminate. This is in accordance with Kovtun et al.[21)] who reported that pair localized exchange of electrons are responsible for conductivity in spinels.

Surface acidity and basicity (Table 3) measurements show that the acidity follows the order aluminate > ferrite > chromites while basicity is in the reverse order. Surface area (Table 2) of chromites and ferrite are comparable which are less than aluminate.

The catalytic activity of $NiCr_2O_4$, $ZnCr_2O_4$, $CuCr_2O_4$, $CuAl_2O_4$, and $CuFe_2O_4$ for the dehydrogenation of ethylbenzene are illustrated in Table 4. The overall conversion of ethylbenzene and the formation of products register an increase with increase of temperature over all the catalysts. However the selectivity to styrene decreases over chromites and ferrite while over aluminate it appears to be unaffected with temperature. The ratio B/T (benzene/toluene) is more than unity over aluminate and less than unity over chromites and ferrite though the actual amount formed over ferrite is significantly low. A small amount of CO_2 and C_2H_4 are formed during the reaction. The former remains constant while the latter increases with temperature over all the catalysts, the increase being exceptionally high over copper aluminate (Table 4).

By correlating the acidity and basicity data with product distribution, it appears that basic sites[22)] over chromites, acidic sites over aluminate, and both acidic and basic sites[23)] over ferrite are involved in the dehydrogenation of ethylbenzene. Benzene and toluene were formed by the cracking of ethylbenzene at C–C and phenyl–C bond respectively. The value of B/T is influenced both by acidic and basic sites. The acidic sites over aluminate favor phenyl–C cracking leading to B/T ratio more than unity while basic sites over chromites favor C–C cracking which makes B/T ratio less than unity. Evolution of ethylene is higher over aluminate than over other catalysts which increases significantly with temperature confirming that it catalyses cracking of phenyl–C bond. The amount of carbon estimated and given in Table 5 follows the order aluminate > chromites > ferrite which is in accordance to the total acidity and basicity values both of which involved in cracking reactions. The formation of CO_2 is attributed to the possible interaction of carbon deposited on the catalysts with lattice oxygen and the constancy of CO_2 formation with increase in temperature indicates that all free oxygen are removed in the lower reaction temperature itself.

The catalytic reaction was carried out continuously for six hours over all catalysts at 823 K (WHSV 2.0 h^{-1}). The results are given in Table 6. The activity of the catalysts remain constant upto 3 h beyond which

Table 6. Change of Yields (mol%) and Conversion of Ethylbenzene (mol%) with Time on Stream[a)]

Time	$NiCr_2O_4$			$ZnCr_2O_4$			$CuCr_2O_4$			$CuFe_2O_4$			$CuAl_2O_4$		
min	1	2	3	1	2	3	1	2	3	1	2	3	1	2	3
90	41.1	34.2	30.8	35.0	30.4	28.0	46.0	32.5	29.0	19.4	17.2	16.5	50.3	21.1	25.1
140	40.5	34.0	29.8	34.6	29.7	27.0	45.1	31.1	27.0	19.2	16.8	15.8	49.1	19.8	22.1
180	40.1	33.1	29.7	34.1	29.1	26.4	44.2	30.9	26.4	19.2	16.9	15.2	48.4	19.1	20.7
240	37.7	30.4	26.1	33.7	28.2	25.3	32.1	25.0	21.6	16.9	16.0	14.1	36.1	18.1	19.4
300	32.1	24.1	21.0	30.1	25.7	23.1	24.4	20.0	16.1	15.1	14.6	13.3	24.5	15.7	15.2
360	26.4	18.7	16.2	27.7	22.1	19.7	16.4	14.7	12.0	11.4	11.0	9.8	13.1	10.7	9.1

a) 1. Ethylbenzene conversion (mol%); 2. Styrene yield (mol%); 3. H_2 (mol%).

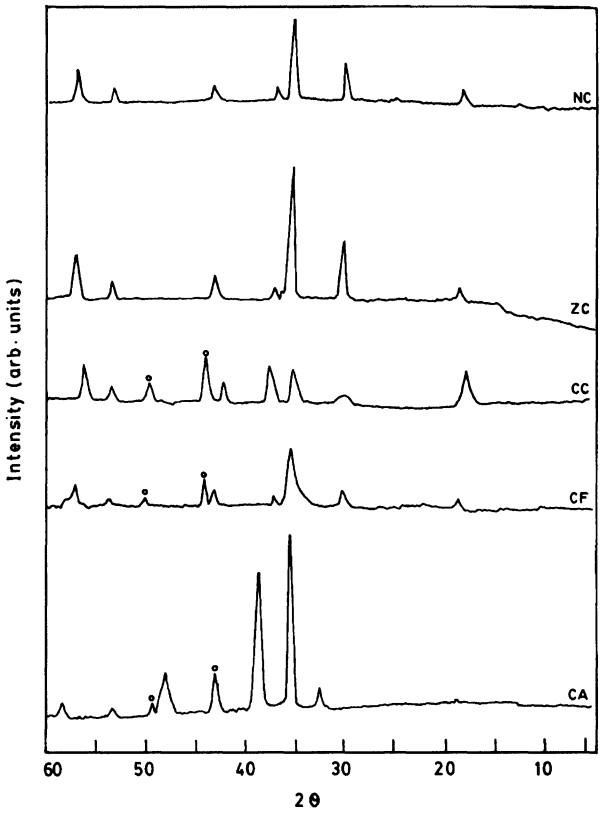

Fig. 4. X-Ray diffractogram of spent catalysts. (0—Cu^0 Phase).

their activity decrease. However the selective formation of styrene is increased over CC, CF, and CA beyond this period. The formation of H_2 is proportional to the styrene yield during the 6 h period. XRD pattern of the spent catalysts (Fig. 4) indicate the appearance of metallic copper phase (Cu^0) over CC, CF, and CA spinels whereas no significant difference is noted in NC and ZC. The Cu^0 phase in CC, CF, and CA is considered to be responsible for the selective formation of styrene and the deactivation of all catalysts is attributed to deposition of coke, which blocks the active centers. Water formation is not observed over all catalysts during the reaction.

References

1) E. H. Lee, *Catal. Rev.*, **8**, 285 (1973).
2) W. W. Kaeding, *Catal. Rev.*, **8**, 307 (1973).
3) B. Delmon, P. A. Jacobs, and G. Poncelet, "Preparation of Catalysts 11," Elsevier, Amsterdam (1979), p. 293.
4) Angeletti, Carlo, and Pepe Franco, *J. Chem. Soc., Faraday Trans. 1*, **74**, 1595 (1978).
5) V. I. Fedecva and I. D. Voinov, *Kinet. Katal.*, **19**, 625 (1978).
6) V. Yu. Prudnikova, *React. Kinet. Catal. Lett.*, **14**, 413 (1980).
7) A. T. Baricevic, B. Brbic, D. Jovanovic, S. Angelov, D. Mehandziev, C. Marinova, and P. Kinilov-Stefanov, *Appl. Catal.*, **47**, 145 (1989).
8) Hightower, *Chem. Eng. Educ.*, **16**, 148 (1982).
9) T. M. Yur'eva, G. K. Boreskov, V. I. Zharkov, L. G. Karakchiev, V. V. Popovskii, and V. A. Chigrina, *Kinet. Katal.*, **9**, 10063 (1968).
10) P. M. Khopkar, J. A. Kulkarni, and V. S. Darshane, *Thermochim. Acta*, **93**, 481 (1985).
11) J. R. Pearce, D. C. Sherwood, M. B. Hall, and J. H. Lunsford, *J. Phys. Chem.*, **84**, 3215 (1980).
12) K. Balasubramanian and V. Krishnasamy, *J. Chem. Soc., Faraday Trans. 1*, **82**, 2665 (1986).
13) J.-C. Wu, C.-S. Chung, C.-L. Ay, and I. Wang, *J. Catal.*, **87**, 98 (1986).
14) M. J. Burger, "Crystal Structure Analysis," Wiley, New York (1960), p. 46.
15) "International Tables for the Determination of Crystal Structure,", Knoch Press, Brimingham (1974), Vol. 2, p. 72.
16) C. K. Jorgenson, "Absorption Spectra and Chemical Binding in Complex," Pergamon Press, New York (1962), pp. 170, 293, and 290.
17) P. Porta, F. S. Stone, and R. G. Turner, *J. Solid State Chem.*, **11**, 135 (1974).
18) H. Weiss., *Z. Phys.*, **132**, 335 (1952).
19) J. J. Freeman and R. M. Friedman, *J. Chem. Soc., Faraday Trans. 1*, **74**, 758 (1978).
20) G. K. Boreskov, Z. Dzevenski, V. V. Popovskii, V. S. Muzykanitov, G. L. Flizarova, C. G. Matuienko, L. M. Plyasova, L. G. Karakchiev, A. A. Ostankovick, and R. A. Sharabina, *Kinet. Katal.*, **11**, 962 (1969).
21) N. M. Kovtun, V. K. Prokopenko, and A. A. Shamyakov, *Solid State Commun.*, **26**, 877 (1978).
22) A. Krause, *Sci. Pharm.*, **38**, 266 (1970).
23) I. Wang, W.-F. Chung, R. -J. Shiau, J.-C. Wu, and C.-S. Chung, *J. Catal.*, **83**, 428 (1983).